10.2 PRODUCT DEVELOPMENT AND EVALUATION FOR THE DUAL-POL WSR-88D RADAR

Kevin Scharfenberg*[1] , Michael Istok[2], Donald Burgess[1], Kevin Manross[1], Richard Murnan[3], and Paul Schlatter[4]

[1] Cooperative Institute for Mesoscale Meteorological Studies, The University of Oklahoma, and NOAA/OAR National Severe Storms Laboratory, Norman, OK
[2] NOAA/National Weather Service Office of Science and Technology, Silver Spring, MD
[3] NOAA/National Weather Service Radar Operations Center, Norman, OK
[4] NOAA/National Weather Service Warning Decision Training Branch, Norman, OK

1. INTRODUCTION

Over the next several years, the U.S. network of WSR-88D weather radars is expected to undergo significant hardware and software upgrades to allow the acquisition of dual-polarimetric ("dual-pol") data. These upgrades are expected to result in improvements to echo classification, precipitation rate estimation, and data quality. The operational utility of dual-pol WSR-88D data was demonstrated during the Joint Polarization Experiment (JPOLE; Ryzhkov et al. 2005; Scharfenberg et al. 2005; Schuur et al. 2003a). Significant improvements are expected to operational decision-making during severe local storms, including flooding (Scharfenberg et al. 2003) and winter storms (Miller and Scharfenberg 2003). During 2006, the National Severe Storms Laboratory (NSSL), acting on behalf of NOAA's National Weather Service (NWS) Radar Operations Center (ROC), conducted a field evaluation of candidate dual-pol WSR-88D products.

Seven dual-pol WSR-88D datasets were distributed to operational users of radar data. These cases were chosen to cover a variety of high-impact weather events, including significant winter storms, severe thunderstorms, mixed precipitation phases, and heavy rainfall. Low-to-moderate-impact weather events were also chosen, including light to moderate rain and snow events. Finally, the data were chosen to include meteorological echoes at various ranges from the radar as well as non-meteorological echoes. Feedback provided by the field evaluators, as well as analyses of the products by a group of evaluators with significant experience in using dual-pol WSR-88D data, were compiled to estimate how operational meteorologists might use the candidate dual-pol products.

* *Corresponding author address:* Kevin Scharfenberg, NSSL/WRDD, 120 David L. Boren Blvd., Norman, OK, 73072.

2. DATA AND METHODOLOGY

2.1. Case Studies

The NSSL WSR-88D (KOUN) was upgraded in 2002 to include dual-pol capabilities. Technical information about KOUN can be found in Doviak et al. (2002), Melnikov et al. (2003), and Melnikov (2004). Although KOUN is not yet considered a full dual-pol prototype, its data may be used to estimate how dual-pol WSR-88D products might be used in the field. Seven KOUN dual-pol WSR-88D archive cases including 31 hours of data were chosen for participants to evaluate:

- 14 May 2003, 0700-1059 UTC
- 10-11 June 2003, 2000-0259 UTC
- 29-30 May 2004, 2300-0359 UTC
- 22 December 2004, 1000-1559 UTC
- 5 January 2005, 0300-0759 UTC
- 28 January 2005, 1603-1859 UTC
- 2 May 2005, 1558-1709 UTC

Summaries of the observed weather were provided to the evaluators on an NSSL web page and are reproduced below. The website also provided participants with additional information and web URLs (where available) pertaining to each case, including surface observations from the Oklahoma Mesonet, atmospheric soundings from KOUN, and constant-pressure maps. When relevant, severe storm reports, severe weather statements and warnings, and rainfall accumulation maps from the Arkansas-Red Basin River Forecast Center were also provided.

The cases were chosen to allow participants to analyze a variety of operationally-significant phenomena, including severe convection, winter weather, mixed precipitation, and heavy rain. Both moderate and high impact events were selected. Ground clutter and other non-meteorological targets were present in several cases, allowing evaluators to comment on situations with data

quality issues. Brief descriptions of each case follow:

14 May 2003

Numerous thunderstorms moved northwest to southeast across the radar range. Many of these thunderstorms were severe with supercell characteristics noted. Large hail was common with the largest report of hail ~13 cm in diameter at 0835 UTC. Thunderstorms moved over the same areas repeatedly leading to a concern for flash flooding. Precipitation echoes were mixed with anomalous propagation and ground clutter at times.

10-11 June 2003

A squall line moved west to east across the radar viewing area, with a trailing region of stratiform rain. During this time period, there were 25 reports of hail between ~2 cm to ~4.5 cm in diameter, 12 reports of wind gusts between 25 and 29 m s^{-1}, and 2 reports of minor flash flooding (near the radar around 11/0200 UTC).

29-30 May 2004

Environmental conditions were strongly favorable for supercell thunderstorms and tornadoes. A supercell thunderstorm moved from extreme western Oklahoma to extreme eastern Oklahoma, crossing the northern Oklahoma City metro area. This storm produced approximately 12 tornadoes and hail as large as ~12 cm in diameter during its life cycle. Wind gusts associated with the storm's rear-flank downdraft were measured at 30 m s^{-1} in the northern part of Oklahoma County at 30/0135 UTC. The storm was also characterized by very strong inflow winds.

22 December 2004

Widespread snowfall was reported with accumulations ranging from ~2.5 to 7.5 cm. A few isolated reports around 10 cm were received to the southeast of KOUN.

5 January 2005

Rain slowly changed over to freezing rain from the northwest during the period. By the end of the data set, freezing rain was falling over the northwest half of the radar coverage area, although a mix with ice pellets was reported with the stronger convective elements. Enough ice accumulated on exposed objects to cause damage to trees and power lines.

28 January 2005

Heavy, wet snow fell across the northwest part of the area, with accumulations from ~7.5 to 20 cm reported. Over the southeast half of the area, light drizzle was punctuated by light showers of ice pellets mixed with a few wet snow flakes.

2 May 2005

A general light rain fell across the area. An isothermal layer near 0ºC was analyzed between 1 and 3 km above ground level, so that the altitudes of the top and bottom of the melting layer varied significantly in space and time in association with the intensity of the precipitation.

2.2. Data Visualization and Interrogation Software

The Warning Decision Support System – Integrated Information (WDSS-II) was the primary data visualization and interrogation software used by the evaluators. WDSS-II is the second generation of a system of tools for the analysis, diagnosis and visualization of remotely sensed weather data (Lakshmanan et al. 2007). WDSS-II was chosen due to its flexibility in displaying experimental data and its unique display and analysis capabilities, such as time- and space-synced multi-panel displays and dynamic cross-sectional and constant-altitude PPI tools.

WDSS-II was distributed to participants via the World Wide Web (the NSSL's ftp server). Users were provided with the WDSS-II software, detailed instructions for installation, and data (both test data and specific cases to analyze). Project administrators provided support via email and a web-based forum for any problems that arose with displaying the data. Technical staffs at the field evaluation sites were able to load WDSS-II and the case data on Linux or Windows platforms.

2.3 Evaluation Groups

Two separate groups concurrently evaluated the products and provided feedback that was

incorporated into a final product evaluation report. External reviews of a draft of the final report from several key agencies involved in WSR-88D research were solicited.

The "Norman" evaluators consisted of several experienced users of KOUN dual-pol products. This group has considerable expertise in the transfer to operations of new data sets, including experience in initial product evaluation for the WSR-88D. This group met twice to draft many of the findings and recommendations for the final product evaluation report.

Meanwhile, comments from a variety of field users were solicited. Feedback was requested from evaluators who frequently use WSR-88D data during their daily weather-related operations. Eight NWS Weather Forecast Offices (WFOs) and one NWS River Forecast Center (RFC) participated on behalf of the U.S. Department of Commerce. Several additional groups represented operational users from other agencies. This group of "field" evaluators provided their feedback via forms on the worldwide web. The Warning Decision Training Branch provided online training materials to these evaluators.

3. BASE DATA AND DERIVED PRODUCTS

3.1. Differential Reflectivity (Z_{DR})

Differential Reflectivity (Z_{DR}) is the ratio of the reflected horizontal and vertical power returns. Z_{DR} is a good indicator of the mean particle shape in the sample volume. In turn, the shape can be a good estimate of the mean particle size. More technical explanations of Z_{DR} and other dual-pol base products can be found in Bringi and Chandrasekar (2001) and Doviak and Zrnić (1993). Z_{DR} values for meteorological echoes generally range from -2 to 6 dB. Isolated values to around 8 dB are possible, particularly associated with large insects. Fig. 1 shows an example Z_{DR} product at 0.5 degree elevation angle, featuring significant returns from thunderstorms with hail and heavy rain, biological scatterers, and significant anomalous propagation (AP).

In general, Z_{DR} is used operationally by meteorologists in concert with other base data to form a four-dimensional model of precipitation type. In thunderstorms, Z_{DR} is quite useful to operations in the detection of hail, of graupel growth associated with updrafts, and of liquid above the regional 0ºC level demarking updraft location. Enhanced Z_{DR} is often noted in the melting layer of precipitation systems and in association with some non-meteorological scatterers. Although rare, Z_{DR} can be used in conjunction with other products to identify lofted tornado debris. Z_{DR} may be useful in understanding the critical microphysical evolution in the rear-flank downdraft region of supercell thunderstorms. Finally, high-altitude electrical charge in the crystal region of some convective systems may be inferred from discontinuities in Z_{DR} between adjacent radials. Because of the small-scale, rapidly-evolving nature of these and

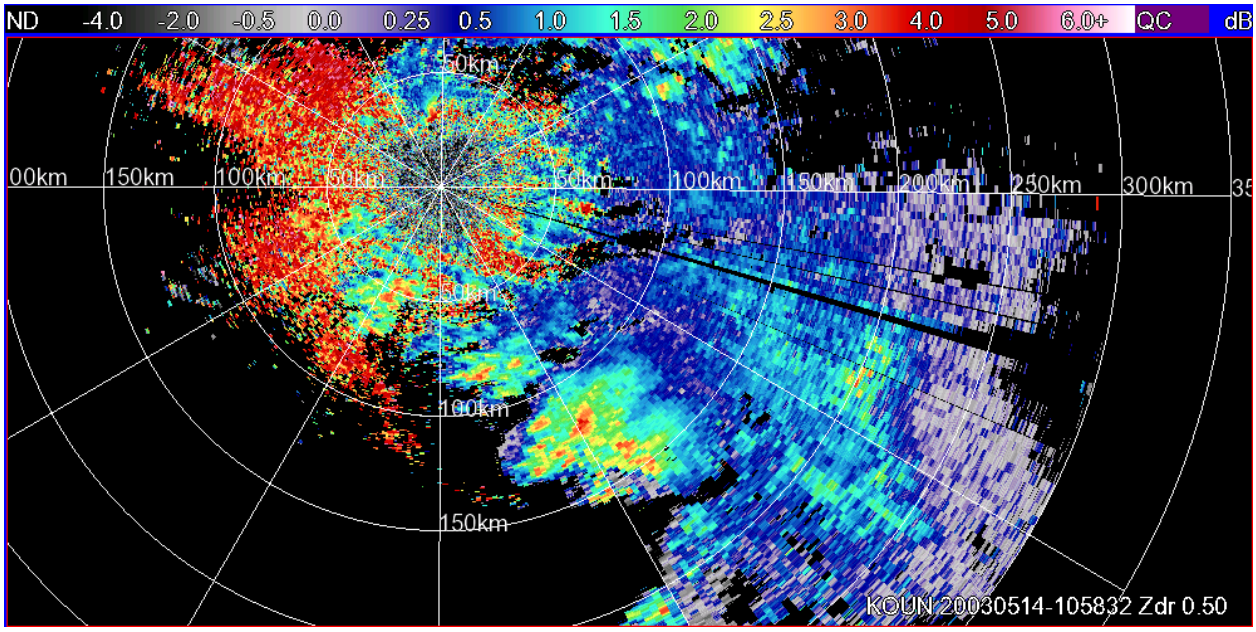

Figure 1. Example differential reflectivity (Z_{DR}) product at 0.5 degree elevation.

other operationally-important features, Z_{DR} data at high spatial resolution and data precision is needed in operational forecasting.

Z_{DR} data can be noisy along the edges of weather echoes in areas of low SNR and in the presence of non-meteorological scatterers, however most evaluators agreed some noise must be displayed to retain important features in weather echoes. A data quality flag might be employed to help users identify questionable data. In addition, user training will be required to help users discriminate meteorologically significant echo from noise.

Because the 0ºC level is critical to interpretation of the Z_{DR} product, evaluators recommended incorporation of temperature data into the displays. For example, the Z_{DR} product may be used to visualize liquid particles in updrafts extending above the regional 0ºC level. To do this, however, the user must first bring up a sounding or numerical model thermodynamic output, determine the altitude of the 0ºC level, then switch back to the radar display and browse up and down through the elevation tilts to find the correct altitude at every point of interest. Instead, the evaluators agreed that temperature data should be available for display directly with the radar data. Additional products could be developed that display the base products on specific constant temperature surfaces (e.g., 0ºC, -10ºC, -20ºC). Furthermore, users would like the ability to browse the radar data in both dynamic constant-altitude plan position indicator (PPI) and dynamic constant-temperature PPI displays.

During thunderstorms, users will want to quickly locate local minima in Z_{DR} at low altitudes for diagnosis of the surface hail threat, as well as local maxima in Z_{DR} at higher altitudes to help locate thunderstorm updrafts. In more stratiform precipitation systems, the Z_{DR} product will be smoother with only a slight maximum associated with the melting layer. Color tables will need to be chosen to account for both situations.

Evaluators agreed that Z_{DR} cannot and will not be used in isolation. In order to successfully develop the mental four-dimensional model of precipitation types and associated weather system structure, users will need to be able to visualize and coordinate 4D patterns in multiple products simultaneously. This will require data to be available at high precision and high spatial resolution. In addition, multi-panel displays will be required to facilitate the development of the 4D conceptual model. Finally, significant training in microphysics and its association to weather system structure will be required. The core group noted that Z_{DR} data will rapidly decay in utility to users beyond 200 km slant range from the radar due to the large volume of each radar gate, though useful identification of significant graupel or lofted liquid in thunderstorm updrafts may be possible at long ranges.

3.2. Correlation Coefficient (ρ_{hv})

The correlation coefficient measures the correlation between the reflected horizontal and vertical power returns. It is a good indicator of regions where there is a mixture of precipitation types, such as rain and snow. Depressed correlation coefficient is also frequently associated with non-meteorological scatterers. Fig. 2 shows a typical ρ_{hv} product at 0.5 degree elevation in a region of significant thunderstorms, rain, and non-meteorological echoes. Values of 0.8 to 1.0 are common in meteorological echoes, though most precipitation echoes will be associated with ρ_{hv} values between 0.95 and 1.0. Because of this, non-linear color tables will be required to allow for interpretation of the ρ_{hv} product. Small changes in data values near 1 are critical and need to be easily discriminated, whereas small data value changes below 0.8 are not as critical to operations.

The ρ_{hv} product is extremely powerful in identifying the altitudes of the top and bottom of the melting layer in precipitation systems. Evaluators found a CAPPI view of ρ_{hv} data was often very helpful in locating the melting layer. In conjunction with other radar data, ρ_{hv} is used to identify regions of mixed precipitation phases and the presence of non-meteorological echoes. Low ρ_{hv} may also be found in regions of Mie scattering, indicative of very large hail when associated with meteorological echoes. The ρ_{hv} product may be used to locate areas of high (low) confidence in a single precipitation type. Finally, ρ_{hv} along with the other base products may be used to identify lofted tornado debris.

Like Z_{DR}. ρ_{hv} is a “noisy” product, particularly at low elevation angles where non-meteorological scatterers are common and along weather echo edges characterized by low SNR. Successful interpretation of this product will also require significant user training. Correlation coefficient

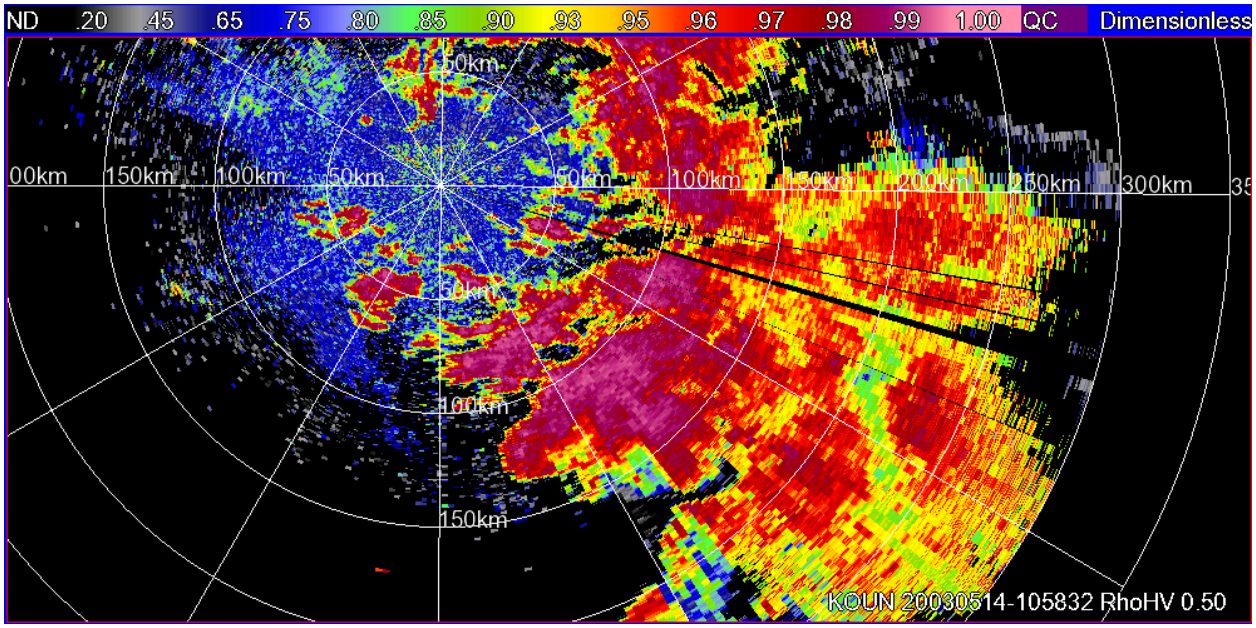

Figure 2. Example correlation coefficient (ρ_{hv}) product at 0.5 degree elevation.

must be used in conjunction with other radar data to successfully form a conceptual 4D model of precipitation type. The new display concepts, incorporation of temperature information, and requirements for data precision and display resolution discussed above also apply to ρ_{hv}. The operational utility of ρ_{hv} also rapidly decays beyond 200 km range, though non-meteorological scatterers at high altitude (i.e., chaff) or a ducted radar beam into terrain may be diagnosed at longer ranges.

3.3. Differential Phase Shift (ϕ_{DP})

The differential phase shift is a comparison of the returned phase differences between the horizontal and vertical pulses. This phase difference is caused by the difference in the number of wave cycles (or wavelengths) along the propagation path for horizontal and vertically polarized waves. It should not to be confused with the Doppler frequency shift, which is caused by the motion of the cloud and precipitation particles. Unlike the differential reflectivity and correlation coefficient, which are all dependent on reflected power, the specific differential phase is a "propagation effect".

In general, little use of differential phase shift is expected in operations. The more important meteorological information is found in the range derivative of this product, the specific differential phase shift (K_{DP}) product. It should be noted that since a smoothing routine on the ϕ_{DP} product is performed in the preprocessor before the creation of the K_{DP} product, the noise filter level decision is critical.

3.4. Specific Differential Phase Shift (K_{DP})

The Specific Differential Phase Shift (K_{DP}) is a derived product mapping the along-radial range derivative of the Differential Phase Shift (ϕ_{DP}). K_{DP} is very strongly related to rain rate. The K_{DP} product as available in May 2006 was evaluated by field users and the core group. An example of K_{DP} at 0.5 degree elevation angle in an area of thunderstorms and heavy rain is shown in Fig. 3. K_{DP} values in weather echoes typically range from -2 to 6 deg km^{-1}, though isolated values above 8 deg km^{-1} have been noted in meteorological echoes.

K_{DP} is primarily used by operational meteorologists to locate areas of heavy rain. Low-amplitude oscillations in K_{DP} are also noted in the melting layer, while high-amplitude noise is typically noted in regions of Mie scattering (i.e., large hail, when associated with weather echoes). Finally, due to dense concentration of very large drops, K_{DP} is often very large at the base of descending wet microbursts (Scharfenberg 2003).

As was the case for Z_{DR} and ρ_{hv}, K_{DP} can be quite noisy. The product will not be used in isolation, but in coordination by meteorologists

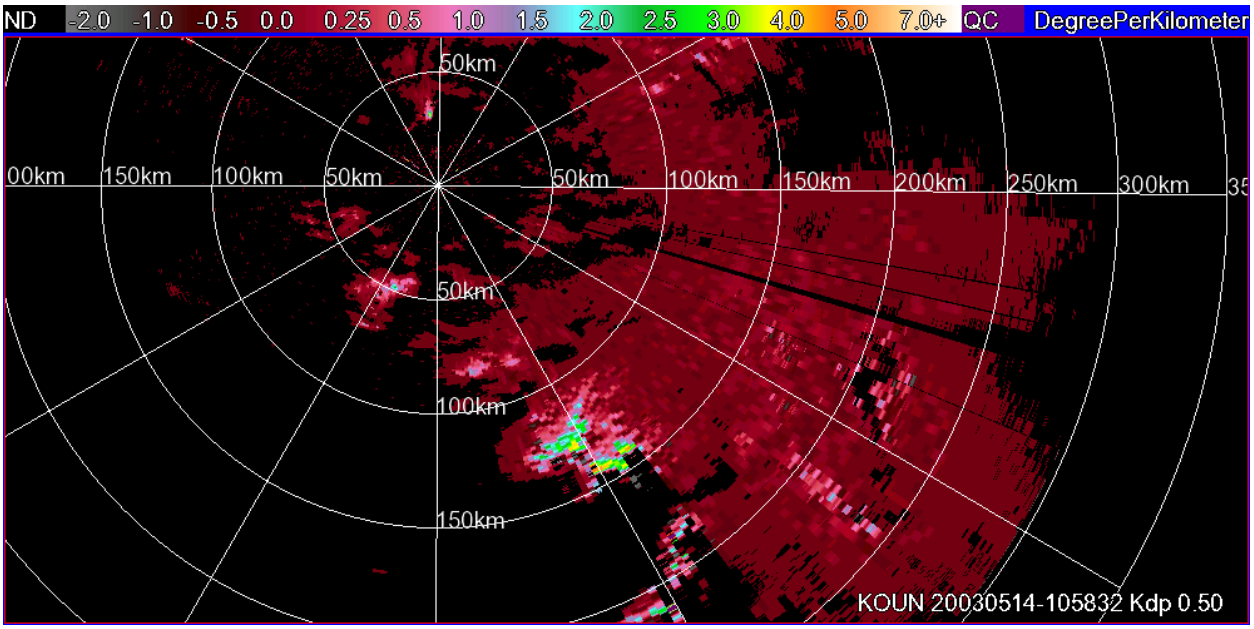

Figure 3. Example specific differential phase (KDP) product at 0.5 degree elevation.

with the other products to develop a 4D conceptual model. The new display concepts, incorporation of temperature information, and requirements for high data precision and display resolution discussed earlier apply to K_{DP} as well. The operational utility of K_{DP} rapidly decays beyond 200 km range, though in a few circumstances, lofted liquid in thunderstorm updrafts may be detected at longer ranges.

4. ALGORITHMS AND DERIVED PRODUCTS

4.1. Hydrometeor Classification Algorithm (HCA)

Hydrometeor classification was a major component of the JPOLE (Schuur et al. 2003b). The dual-pol Hydrometeor Classification Algorithm (HCA) product available as of May 2006 and described in Scharfenberg (2006a) was evaluated. An example of HCA output during a mixture of widespread thunderstorms and non-precipitation echoes is shown in Fig. 4. The HCA algorithm is a fuzzy logic method of calculating the most probable dominant scatterer type in each sample volume. A single category is displayed at every gate at every elevation angle at the same resolution as the base data. The HCA interacts with a melting layer detection algorithm (MLDA), as described in Giangrande et al. (2005). The MLDA does not produce any output that could be directly evaluated, though the sub-algorithm's general performance could be estimated by examination of the output of the HCA.

The "rain/hail" category was useful to operations as a "flag" of locations where the meteorologist should further scrutinize the base products. This category seems to be reliable enough for use by non-meteorologists. Some evaluators suggested a probabilistic interest field for hail derived from the HCA algorithm would be useful to operations.

The evaluators believe HCA will also be useful to operational users in the delineation between precipitation and non-precipitation echoes and in identification of questionable data. A full analysis of the HCA and MLDA performance in the cases studied and recommendations for future improvements are beyond the scope of this evaluation, though it appears most incorrect HCA classifications are tied to challenges in the detection of the melting layer by the MLDA, as well as some possible data calibration issues. The MLDA requires sufficient coverage of precipitation echoes at elevation angles between 4 and 10 degrees to be successful (Giangrande et al. 2005).

In general, the HCA and MLDA are very complex algorithms individually with numerous contingencies, and they interact with each other in a complicated manner. A significant training effort for users to understand the strengths and limitations of the algorithms will be required. Users

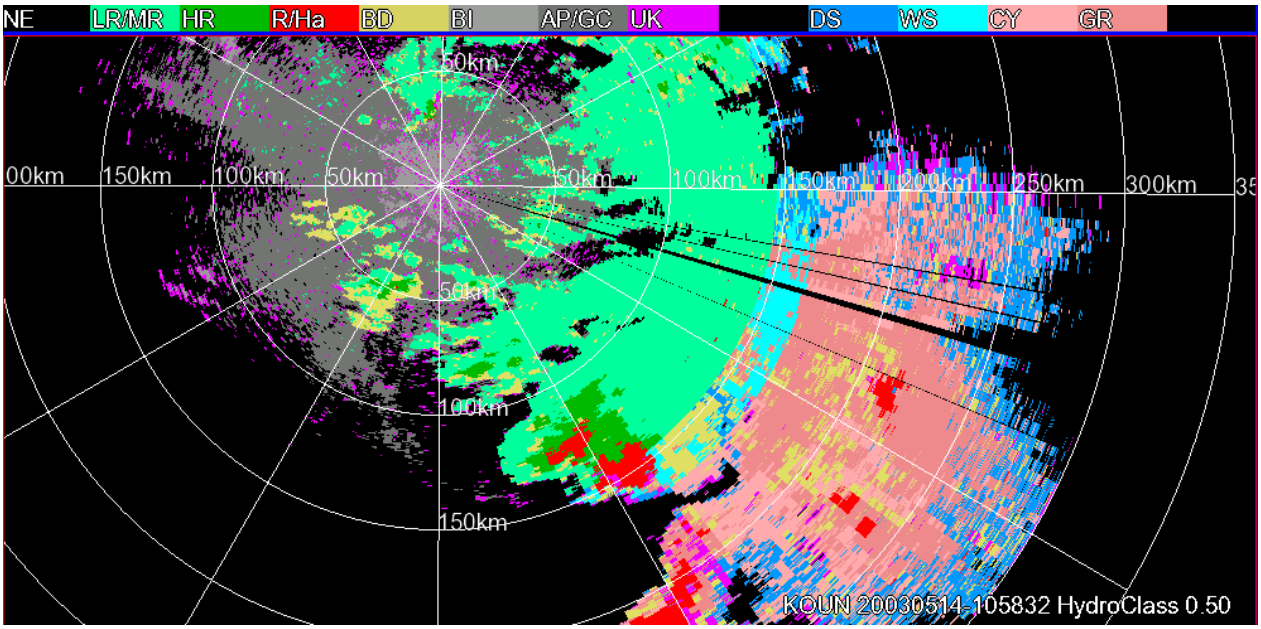

Figure 4. Example output from the hydrometeor classification algorithm product at 0.5 degree elevation. In the color code: NE=no echo, LR/MR=light/moderate rain, HR=heavy rain, R/Ha=rain/hail, BD=big drops, BI=biological scatterers, AP/GC=anomalous propagation/ground clutter, UK=unknown, DS=dry snow, WS=wet snow, CY=crystals, and GR=graupel.

will need to understand some unphysical output must be expected due to radar sampling limitations. Use of adaptable parameters will be critical for success, though it is currently unclear exactly how this will be done operationally. Incorporation of user inputs and data from automated sources, such as the RUC model, will have to be explored. Further testing and evaluation of these concepts is required, including periodic code review and testing.

Despite the remaining challenges, HCA and MLDA capabilities may be very helpful in forecast operations, particularly in winter storms (Scharfenberg and Maxwell 2003). Like the base products, the HCA will not be used alone, but in concert with other products. Confidence in the utility of the HCA product decays beyond 200 km slant range due to the limitations in the base data previously discussed.

4.2. "Filtered Reflectivity" Product

The filtered reflectivity product as available in May 2006 was evaluated. The filtered reflectivity attempts to remove all non-precipitation returns from the display, using output from the HCA.

Although evaluators agreed the filtered reflectivity product was effective at removing non-precipitation echoes, it is not expected this product will be used a great deal by NWS forecasters. Meteorologists take cues from significant non-precipitating scatterers (i.e., clear-air boundaries) and are trained to interpret and mentally filter noise. Some interests require all weather-related echoes greater than 30 dBZ to be displayed, along with the retention of clear-air boundaries. The former is possible with the filtered reflectivity product but the latter requirement is far more challenging. Other external users may find benefit from a filtered reflectivity product.

4.3. Quantitative Precipitation Estimation (QPE) Algorithms

The JPOLE data suggest considerable improvement may be made to operational WSR-88D QPE products (Ryzhkov 2003). 20 QPE algorithm products, as available in May 2006 and described in Scharfenberg (2006c) were evaluated. These products included instantaneous rain rate, and accumulation estimates for 1 hour, 3 hour and storm total rainfall.

Evaluators agreed that major improvements to remote QPE using a dual-pol WSR-88D network are likely, particularly in flash flood warning decision-making and forecasting. This will also enhance general runoff and flood forecasting, as

well as longer-term flash flood guidance. The evaluation found there is a wide variety of radar QPE output needs within the hydrometeorological community. These needs can vary significantly depending on the user, application, or algorithm. Most evaluators preferred the current method of radar-output polar products, at 8-bit precision and at the spatial resolution of the base reflectivity data, with any smoothing or averaging done by individual applications, algorithms, and institutions external to the radar data stream

The evaluated dual-pol QPE products were found to be "noisy" in some cases. This is a substantial change from the current QPE products available in operations and significant training will be required for interpretation.

Instantaneous rainfall rate information was found to be potentially useful in flash flood warning decision-making. These products can be used to diagnose a sudden increase in precipitation rate or to anticipate the movement of a heavy rainfall area over a flash flood-prone location.

Due to sampling limitations, QPE products beyond 200 km slant range from the radar are generally not useful to operations (Giangrande and Ryzhkov 2003).

5. SUMMARY

The upcoming WSR-88D upgrade to include dual-pol capability presents many opportunities and many challenges. The most significant challenges involve user training and visualization. Meteorologists interpreting the data will need to be able to associate patterns in several base products, including reflectivity, to form a 4D conceptual model of atmospheric phenomena.

Understanding the base data will require not only radar interpretation training, but related training in microphysics, thermodynamics, storm structure, and so on. The algorithms are quite complex which will require further training for understanding. Visualization software will have to be tailored to allow the user to quickly browse through large volumes of data that arrive very quickly.

Despite the challenges, significant improvements to situation awareness can be gained by using dual-pol WSR-88D data. Users can gain significant understanding of the microphysical structure of precipitating systems, allowing for a better conceptual model of evolving, high-impact weather systems. Significant advances in data quality, hydrometeor classification, and quantitative precipitation estimation can be expected as these products evolve and reach the field.

Acknowledgments: The valuable feedback from the evaluators and external reviewers form the basis of this work. This paper would not have been possible without the dedicated work of the scientists, IT staff, and engineers who collect, process, and distribute KOUN data.

This extended abstract was prepared by Kevin Scharfenberg with funding provided by NOAA/Office of Oceanic and Atmospheric Research under NOAA-University of Oklahoma Cooperative Agreement #NA17RJ1227, U.S. Department of Commerce. The statements, findings, conclusions, and recommendations are those of the author(s) and do not necessarily reflect the views of NOAA or the U.S. Department of Commerce.

REFERENCES

Bringi, V. N., and V. Chandrasekar, 2001: *Polarimetric Doppler Weather Radar: Principles and Applications.* Cambridge University Press, Cambridge, UK, 662 pp.

Doviak, R. J., and D. S. Zrnić, 1993: *Doppler Radar and Weather Observations, 2nd ed.* Academic Press, San Diego, CA, 562 pp.

————, J. Carter, V. Melnikov, and D. S. Zrnić, 2002: Modification to the Research WSR-88D to Obtain Polarimetric Data, NOAA/NSSL Report, 49 pp.

Giangrande, S., and A. V. Ryzhkov, 2003: The quality of rainfall estimation with the polarimetric WSR-88D radar as a function of range. *Preprints, 31st Intl. Conf. on Radar Meteor.,* Seattle, WA, USA, Amer. Meteor. Soc., 357–360.

————, ————, and J. Krause, 2005: Automatic Detection of the Melting Layer with a Polarimetric Prototype of the WSR-88D Radar. *Preprints, 32nd Conf. on Radar*

Meteor., Albuquerque, NM, Amer. Meteor. Soc., CD-ROM, 11R.2.

Lakshmanan, V., T. Smith, G. J. Stumpf, and K. Hondl, 2007: The Warning Decision Support System - Integrated Information (WDSS-II). *Weather and Forecasting*, accepted for publication.

Melnikov, V. M., 2004: Simultaneous Transmission Mode for the Polarimetric WSR-88D. Report of the National Severe Storms Laboratory, 84 pp.

————, V. M., D. S. Zrnić, R. J. Doviak, and J. K. Carter, 2003: Calibration and Performance Analysis of NSSL's Polarimetric WSR-88D, NOAA/NSSL Report, 77 pp.

Miller, D. J., and K. Scharfenberg, 2003: The use of polarimetric radar data in the winter weather warning decision-making process: A case study. *Preprints, 31st Intl. Conf. on Radar Meteor.,* Seattle, WA, Amer. Meteor. Soc., 976–979.

Ryzhkov, A., 2003: Rainfall Measurements with the Polarimetric WSR-88D Radar, NOAA/NSSL Report, 99 pp.

————, T. J. Schuur, D. W. Burgess, P. L. Heinselman, S. E. Giangrande, and D. S. Zrnić, 2005: The Joint Polarization Experiment: Polarimetric rainfall measurements and hydrometeor classification. *Bull. Amer. Meteor. Soc.*, **86**, 809–824.

Scharfenberg, K., 2006a: A functional description of the NSSL polarimetric hydrometeor classification algorithm. Report of the National Severe Storms Laboratory, 9 pp.

————, 2006b: A functional description of the NSSL polarimetric quantitative precipitation estimation algorithm. Report of the National Severe Storms Laboratory, 6 pp.

————, 2003: Polarimetric radar signatures in microburst-producing thunderstorms. Preprints, *31st Int. Conf. on Radar Meteorology,* Seattle, WA, Amer. Meteor. Soc., 581–584.

———— and E. Maxwell, 2003: Operational use of a hydrometeor classification algorithm to detect the snow melting level. *Preprints, 31st Intl. Conf. on Radar Meteor.,* Seattle, WA, Amer. Meteor. Soc., 639–641.

————, D. J. Miller, T. J. Schuur, P. T. Schlatter, S. E. Giangrande, V. M. Melnikov, D. W. Burgess, D. L. Andra, Jr., M. P. Foster, and J. M. Krause, 2005: The Joint Polarization Experiment: Polarimetric radar in forecasting and warning decision-making, *Weather and Forecasting,* **20,** 775–788.

————, M. P. Foster, and D. L. Andra, 2003: Operational uses of polarimetric data in severe local storm prediction. *Preprints, 31st Intl. Conf. on Radar Meteor.,* Seattle, WA, Amer. Meteor. Soc., 632–634.

Schuur, T., P. Heinselman, and K. Scharfenberg, 2003a: Overview of the Joint Polarization Experiment (JPOLE), NOAA/NSSL Report, 38 pp.

————, A. Ryzhkov, and P. Heinselman, 2003b: Observations and Classification of Echoes with the Polarimetric WSR-88D Radar, NOAA/NSSL Report, 45 pp.